A segmented total energy detector (sTED) for (n, γ) cross section measurements at n_TOF EAR2

V. Alcayne[1], D. Cano-Ott[1], J. Garcia[1], E. González-Romero[1], T. Martínez[1], E. Mendoza[1], A. Sánchez[1], J. Plaza[1], J. Balibrea-Correa[2], A. Casanovas[2], C. Domingo-Pardo[2], J. Lerendegui-Marco[2], O. Aberle[2], S. Altieri[3,4], S. Amaducci[5], H. Amar Es-Sghir[6], J. Andrzejewski[7], V. Babiano-Suarez[8], M. Bacak[2], J. Balibrea[8], S. Bennett[9], A. P. Bernardes[2], E. Berthoumieux[10], D. Bosnar[11], M. Busso[12,13], M. Caamaño[14], F. Calviño[15], M. Calviani[2], D. Cano-Ott[1], A. Casanovas[8], D. M. Castelluccio[16,17], F. Cerutti[2], G. Cescutti[18,19], S. Chasapoglou[20], E. Chiaveri[2,9], P. Colombetti[21,22], N. Colonna[23], P. C. Console Camprini[16,17], G. Cortés[15], M. A. Cortés-Giraldo[24], L. Cosentino[5], S. Cristallo[12,25], M. Di Castro[2], D. Diacono[23], M. Diakaki[20], M. Dietz[26], C. Domingo-Pardo[8], R. Dressler[27], E. Dupont[10], I. Durán[14], Z. Eleme[28], S. Fargier[2], B. Fernández-Domínguez[14], P. Finocchiaro[5], S. Fiore[16,29], V. Furman[30], F. García-Infantes[6], A. Gawlik-Ramięga[7], G. Gervino[21,22], S. Gilardoni[2], E. González-Romero[1], C. Guerrero[24], F. Gunsing[10], C. Gustavino[29], J. Heyse[31], D. G. Jenkins[32], E. Jericha[33], A. Junghans[34], Y. Kadi[2], T. Katabuchi[35], I. Knapová[36], M. Kokkoris[20], Y. Kopatch[30], M. Krtička[36], D. Kurtulgil[37], I. Ladarescu[8], C. Lederer-Woods[38], J. Lerendegui-Marco[8], G. Lerner[2], A. Manna[17,39], T. Martínez[1], A. Masi[2], C. Massimi[17,39], P. Mastinu[40], M. Mastromarco[23,41], F. Matteucci[18,19], E. A. Maugeri[27], A. Mazzone[23,42], E. Mendoza[1], A. Mengoni[16,17], V. Michalopoulou[20,2], P. M. Milazzo[18], R. Mucciola[12,13], F. Murtas[†43], E. Musacchio-Gonzalez[40], A. Musumarra[44,45], A. Negret[46], A. Oprea[46], P. Pérez-Maroto[24], N. Patronis[28], J. A. Pavón-Rodríguez[24], M. G. Pellegriti[44], J. Perkowski[7], C. Petrone[46], L. Piersanti[12,25], E. Pirovano[26], S. Pomp[47], I. Porras[6], J. Praena[6,2], N. Protti[3,4], J. M. Quesada[24], T. Rauscher[48], R. Reifarth[37], D. Rochman[27], Y. Romanets[49], F. Romano[44], C. Rubbia[2], A. Sánchez[1], M. Sabaté-Gilarte[2], P. Schillebeeckx[31], D. Schumann[27], A. Sekhar[9], A. G. Smith[9], N. V. Sosnin[38], M. Spelta[17,39], M. E. Stamati[28], G. Tagliente[23], A. Tarifeño-Saldivia[15], D. Tarrío[47], N. Terranova[16,43], P. Torres-Sánchez[6], S. Urlass[34,2], S. Valenta[36], V. Variale[23], P. Vaz[49], D. Vescovi[37], V. Vlachoudis[2], R. Vlastou[20], A. Wallner[50], P. J. Woods[38], T. Wright[9], P. Žugec[11], and the n_TOF Collaboration

[1]Centro de Investigaciones Energéticas Medioambientales y Tecnológicas (CIEMAT), Spain
[2]Instituto de Física Corpuscular, CSIC - Universidad de Valencia, Spain
[3]European Organization for Nuclear Research (CERN), Switzerland
[4]Istituto Nazionale di Fisica Nucleare, Sezione di Pavia, Italy
[5]Department of Physics, University of Pavia, Italy
[6]INFN Laboratori Nazionali del Sud, Catania, Italy
[7]University of Granada, Spain
[8]University of Lodz, Poland
[9]University of Manchester, United Kingdom
[10]CEA Irfu, Université Paris-Saclay, F-91191 Gif-sur-Yvette, France
[11]Department of Physics, Faculty of Science, University of Zagreb, Zagreb, Croatia
[12]Istituto Nazionale di Fisica Nucleare, Sezione di Perugia, Italy
[13]Dipartimento di Fisica e Geologia, Università di Perugia, Italy
[14]University of Santiago de Compostela, Spain
[15]Universitat Politècnica de Catalunya, Spain
[16]Agenzia nazionale per le nuove tecnologie (ENEA), Italy
[17]Istituto Nazionale di Fisica Nucleare, Sezione di Bologna, Italy
[18]Istituto Nazionale di Fisica Nucleare, Sezione di Trieste, Italy
[19]Department of Physics, University of Trieste, Italy
[20]National Technical University of Athens, Greece
[21]Istituto Nazionale di Fisica Nucleare, Sezione di Torino, Italy
[22]Department of Physics, University of Torino, Italy
[23]Istituto Nazionale di Fisica Nucleare, Sezione di Bari, Italy
[24]Universidad de Sevilla, Spain
[25]Istituto Nazionale di Astrofisica - Osservatorio Astronomico di Teramo, Italy
[26]Physikalisch-Technische Bundesanstalt (PTB), Bundesallee 100, 38116 Braunschweig, Germany
[27]Paul Scherrer Institut (PSI), Villigen, Switzerland
[28]University of Ioannina, Greece
[29]Istituto Nazionale di Fisica Nucleare, Sezione di Roma1, Roma, Italy
[30]Joint Institute for Nuclear Research (JINR), Dubna, Russia

[31]European Commission, Joint Research Centre (JRC), Geel, Belgium
[32]University of York, United Kingdom
[33]TU Wien, Atominstitut, Stadionallee 2, 1020 Wien, Austria
[34]Helmholtz-Zentrum Dresden-Rossendorf, Germany
[35]Tokyo Institute of Technology, Japan
[36]Charles University, Prague, Czech Republic
[37]Goethe University Frankfurt, Germany
[38]School of Physics and Astronomy, University of Edinburgh, United Kingdom
[39]Dipartimento di Fisica e Astronomia, Università di Bologna, Italy
[40]INFN Laboratori Nazionali di Legnaro, Italy
[41]Dipartimento Interateneo di Fisica, Università degli Studi di Bari, Italy
[42]Consiglio Nazionale delle Ricerche, Bari, Italy
[43]INFN Laboratori Nazionali di Frascati, Italy
[44]Istituto Nazionale di Fisica Nucleare, Sezione di Catania, Italy
[45]Department of Physics and Astronomy, University of Catania, Italy
[46]Horia Hulubei National Institute of Physics and Nuclear Engineering, Romania
[47]Uppsala University, Sweden
[48]Department of Physics, University of Basel, Switzerland
[49]Instituto Superior Técnico, Lisbon, Portugal
[50]Australian National University, Canberra, Australia

Abstract.
The neutron time-of-flight facility n_TOF is characterised by its high instantaneous neutron intensity, high-resolution and broad neutron energy spectra, specially conceived for neutron-induced reaction cross section measurements. Two Time-Of-Flight (TOF) experimental areas are available at the facility: experimental area 1 (EAR1), located at the end of the 185 m horizontal flight path from the spallation target, and experimental area 2 (EAR2), placed at 20 m from the target in the vertical direction. The neutron fluence in EAR2 is ~300 times more intense than in EAR1 in the relevant time-of-flight window. EAR2 was designed to carry out challenging cross-section measurements with low mass samples (approximately 1 mg), reactions with small cross-sections or/and highly radioactive samples. The high instantaneous fluence of EAR2 results in high counting rates that challenge the existing capture systems. Therefore, the sTED detector has been designed to mitigate these effects. In 2021, a dedicated campaign was done validating the performance of the detector up to at least 300 keV neutron energy. After this campaign, the detector has been used to perform various capture cross section measurements at n_TOF EAR2.

1 Introduction

The neutron time-of-flight facility n_TOF at CERN has been dedicated mostly to measurements of neutron-induced cross sections of interest mainly in nuclear technology and astrophysics. Since 2014, the Experimental ARea 2 (EAR2) [1] located in the vertical direction at 20 m from the spallation target is operational. The neutron fluence in EAR2 is ~300 times more intense in the relevant time-of-flight window than the Experimental ARea 1 (EAR1) located at 185 m [2], since it has a ~30 times larger neutron fluence and a ~10 times shorter flight times. EAR2 was designed to carry out challenging cross-section measurements with low mass samples (approximately 1 mg), reactions with small cross-sections and/or highly radioactive samples [3–7].

Two capture cross sections measurements were performed in the EAR2 [7, 8] with the conventional C_6D_6 detectors available at n_TOF; the so-called BICRON (0.621 L of liquid) [9] and Legnaro (1.0 L of liquid) [10] detectors that have been extensively used and validated in EAR1. As described in Ref. [11] these detectors in EAR2 required considerable corrections that increased with the energy of the neutron and did not allow to measure cross sections at neutron energies higher than some keVs.

In fact, the increase in more than two orders of magnitude of the instantaneous flux leads to an equivalent increase in the counting rates in the detectors, as presented in Fig. 1. The high counting rates of the EAR2 can produce pile-up effects and gain shifts in the conventional C_6D_6 detectors of n_TOF (BICRON and Legnaro). Two different gain shifts were observed: constant gains shift due to high constant counting rates and gain shifts that are produced by instantaneous high counting rates. At n_TOF, neutrons are produced in the spallation reactions induced by a 20 GeV/c proton beam in a massive lead target. In these reactions, a particle-flash of relativistic charged particles, high energy neutrons and prompt γ-rays coming with very short time-of-flight is also produced, which arrives at the experimental areas at very short times ($<1\mu$s). This particle-flash in EAR2 produces gain shifts and saturation effects in the PMTs that can affect the performance and reliability of the detectors.

In order to address EAR2 challenges, a new detector has been developed, the Segmented Total Energy Detector (sTED). This detector has an active volume of C_6D_6 liquid of 0.044 L. The drawing of the detector is presented in Figure 2 and the estimated efficiencies of the detector are given in Table 1.

The sTED detector is designed to overcome all the previous problems that suffer the conventional n_TOF C_6D_6 detectors. Thanks to a smaller active volume, the counting rate is considerably smaller, leading to a reduction of pile-

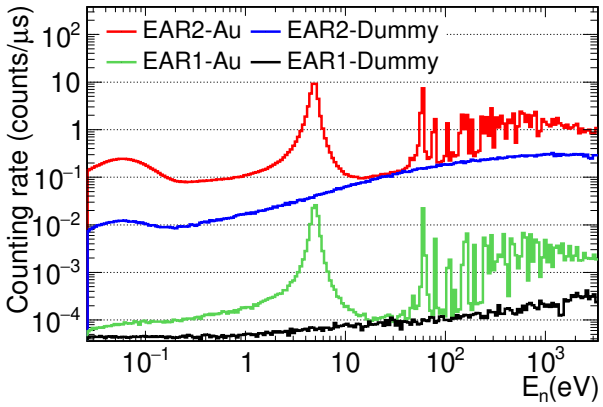

Figure 1. The counting rates obtained in the experimental EAR1 (EAR1-Au) and EAR2 (EAR2-Au) for a BICRON detector with a threshold of 0.15 MeV located at approximately 10 cm from a ^{197}Au sample of 2 cm diameter and 100 μm thickness. Also, the counting rate of the beam-on background obtained with a dummy sample are presented for the EAR1 (EAR1-Dummy) and the EAR2 (EAR2-Dummy).

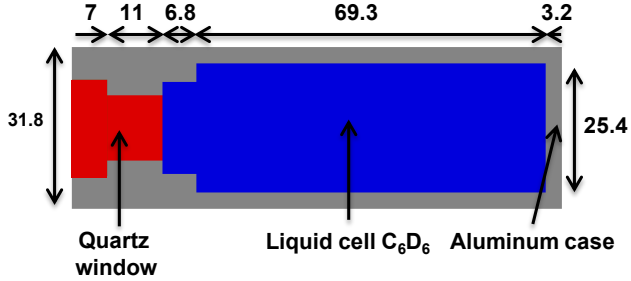

Figure 2. Drawing of the sTED detector with the different components and their size in millimetres.

Table 1. The detection efficiencies for C_6D_6 detectors in percentage to the isotropic emission of γ-rays of 1 MeV and 5 MeV and the deexcitation γ-ray cascades of ^{197}Au and ^{240}Pu. The efficiencies were calculated with Geant4 simulations [12] with a detection threshold of 0.15 MeV and the detectors were placed at 5 cm from the γ-ray sources.

	1 MeV γ-rays	5 MeV γ-rays	^{197}Au cascades	^{240}Pu cascades
Legnaro	3.39	2.20	4.77	6.09
BICRON	2.72	1.83	3.86	4.89
sTED	0.24	0.21	0.35	0.43

up effects and gain shifts. To further reduce possible gain shifts a Hamamatsu R11265U PMT 26x26 mm model has been employed, with features a borosilicate window and photocathodes made of super bialkali (SBA) specifically designed for high counting rates. The use of a smaller active volume and PMT also reduce the possible undesirable effects of the particle-flash.

At the moment there are 9 sTED modules built, that can be used separately or in cluster mode, see Figure 3. Funding has been already found to buy 27 more sTED modules, thus the total number of sTED modules would be 36.

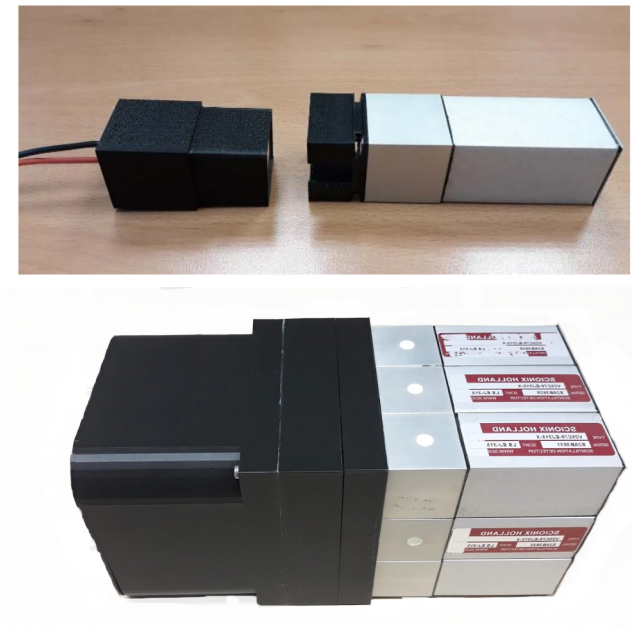

Figure 3. Picture of one sTED module (top). Picture of one sTED cluster made of 9 sTED modules (bottom).

As previously mentioned, EAR2 is designed to perform capture measurements of samples with low mass or/and small cross section. However, one of the main limitations to perform capture measurements in this area is the signal to beam-on background ratio (SBR), increasing considerably the systematic uncertainties due to the subtraction of this background component [11]. In 2021 to study this background, dedicated measurements were performed at different distances from the centre of the beam with BICRON detectors. As presented in Fig. 4, the beam-on background measured at 5, 15 and 30 cm are practically the same for neutron energies higher than 1 eV. The efficiency to detect the γ-ray capture cascade with a detector at 5 cm is approximately a factor of 10 higher than with a detector at 15 cm. Therefore, if we consider only the beam-on background, the SBR is improved approximately by a factor of 10 if we place the detector at 5 cm instead of 15 cm. The conventional C_6D_6 detectors can not be placed close (i.e < 15 cm) to the beam due to high pile-up effects. However the sTED can be placed at distances from the beam as close as 5 cm, thus increasing the SBR.

2 Characterization of the detector in 2021

In 2021 a dedicated campaign was performed to validate the sTED detector at EAR2. The first step of the work was to characterize the sTED response with various γ-ray sources (^{137}Cs, ^{88}Y and Am-Be) and Monte Carlo simulations performed with Geant4. The detector resolution and the signal amplitude to energy conversion were obtained by comparing the simulated response and the response obtained experimentally. In Fig. 5 the match between the

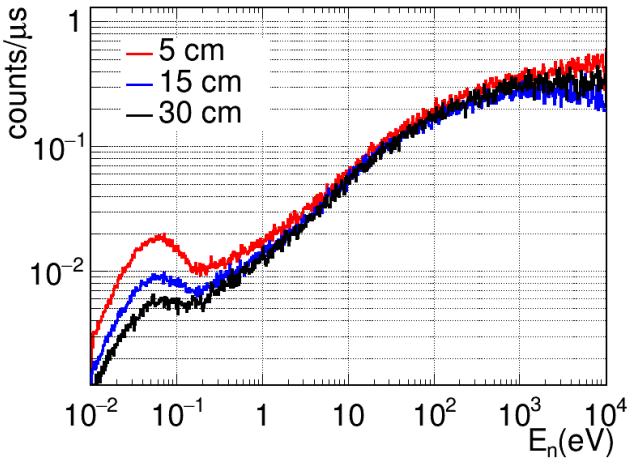

Figure 4. The counting rates obtained for a BICRON detector in a beam-on measurement with a dummy (i.e. with a layer of Mylar of 10 μm). sample at different distances from the centre of the beam.

simulations and the experimental results are presented for an ^{88}Y γ-ray source. To finally validate the behaviour of

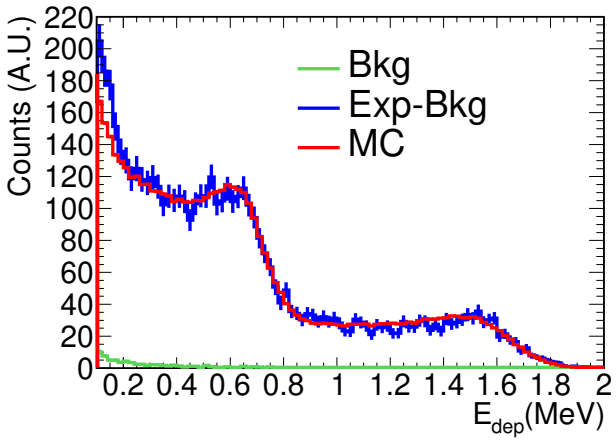

Figure 5. Geant4 simulations for an ^{88}Y γ-ray sources (MC) compared with the experimental results with the background subtracted (Exp-Bkg) after the calibration.

the detector, the yield for an ^{197}Au sample of 2 cm diameter and 0.1 mm thickness is compared with the yield obtained with the evaluated data of JEFF-3.3 [13]. The experimental yield is calculated by dividing the counting rate in the sTED detector as a function of the neutron energy by the neutron fluence of the EAR2, after subtracting the different background components affecting the measurement. This experimental yield is compared with the yield obtained with the JEFF-3.3 cross section convoluted with the Resolution Function (RF) of the EAR2 in Fig. 6. The two yields are normalised in the first resonance at 4.9 eV, the RF and fluence of the EAR2 used for this work are preliminary [14]. In Figure 7 the comparison between the experimental yield and the one of JEFF-3.3 are presented with 10 bins per decade. The shape of the two yields are compatible and the differences observed can be due to the

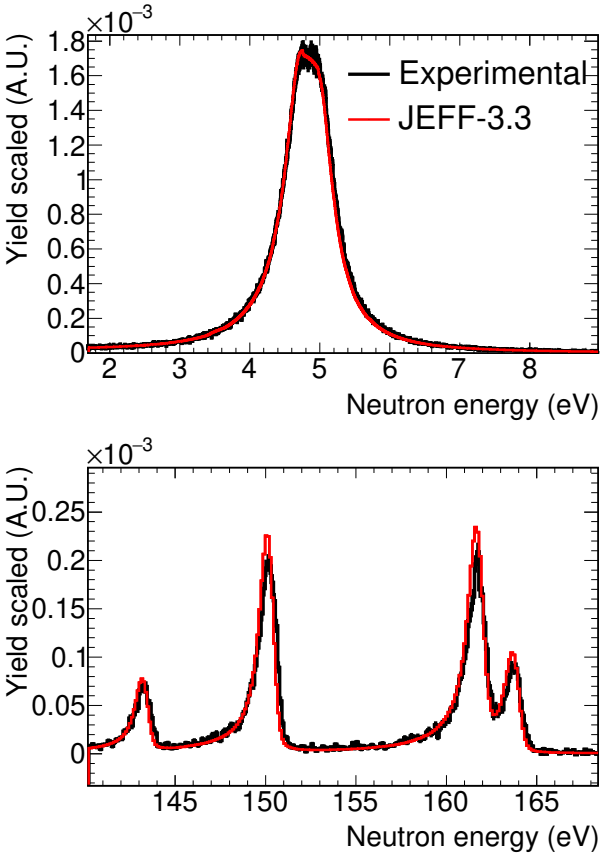

Figure 6. The experimental capture yield obtained for an sTED detector with a ^{197}Au sample (Experimental) compared with the yield obtained for the JEFF-3.3 nuclear data library (JEFF-3.3) for various resonances.

statistical uncertainties or to the uncertainties in the preliminary fluence or RF. At energies higher than 300 keV there are considerable differences, these differences can be due to the opening of the (n,n') inelastic reaction channels. The cross section for inelastic reaction in ^{197}Au is significantly higher than the capture cross section at energies above 300 keV.

3 The sTED capture campaigns

In 2022 nine sTEDs detectors were used to measure the capture cross section of ^{79}Se and ^{94}Nb at a distance of 4.5 cm from the sample, see Figure 8 [15, 16]. The results obtained in these measurements are very promising and the setup has been also used to perform the capture cross section measurements of ^{160}Gd and ^{94,95,96}Mo.

4 Future work and conclusions

The different limitations observed with the conventional C_6D_6 detectors at n_TOF EAR2 to perform capture measurements have been studied and the sTED detector was designed to overcome them. The sTED is made with a small active volume per detector and a PMT optimized for high instantaneous counting rates. In 2021, a dedicated

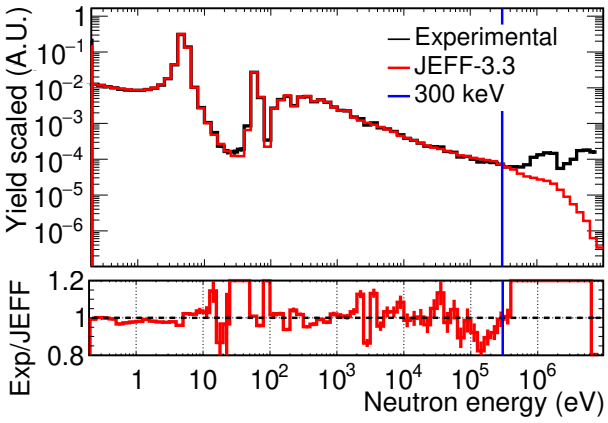

Figure 7. The experimental capture yield obtained for an sTED detector with a ^{197}Au sample (Experimental) compared with the yield obtained for the JEFF-3.3 nuclear data library (JEFF-3.3) with 10 bins per decade.

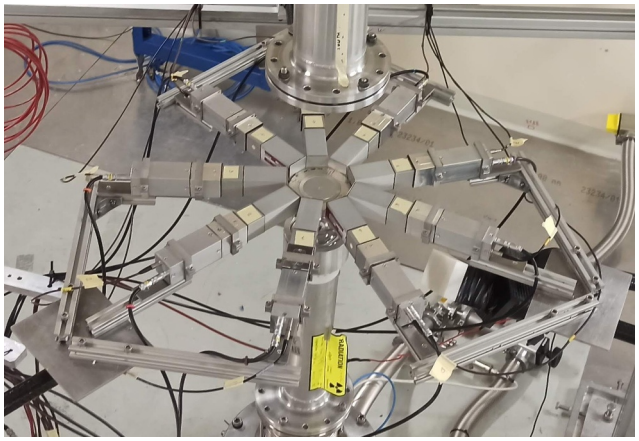

Figure 8. 9 sTEDs detectors in the configuration used to measure the capture cross section of ^{79}Se and ^{94}Nb.

campaign at EAR2 was performed to validate the sTED detector. In this measurement, the capture yield obtained for an ^{197}Au sample was compatible with the JEFF-3.3 capture cross section up to the inelastic threshold at 300 keV. In the short term, an experimental campaign would be performed with 9 sTED detectors, to make the same measurement with higher statistics and using the evaluated version of the fluence and the RF of EAR2. The sTED detector has been already used to perform capture measurements on ^{79}Se, ^{94}Nb, ^{160}Gd and ^{94,65,96}Mo. There is a final paper on the sTED detector in preparation.

5 Acknowledgments

This work was supported in part by the I+D+i grant PGC2018-096717-B-C21 funded by MCIN/AEI/10.13039/501100011033 and by the European Commission H2020 Framework Programme project SANDA (Grant agreement ID: 847552).

References

[1] C. Weiss et al., Nucl. Instrum. Meth. A 799, 90 (2015)
[2] Guerrero, C. et al. Eur. Phys. J. A 49, 27 (2013)
[3] M. Barbagallo et. al., Phys. Rev. Let., 117, 152701 (2016)
[4] M. Sabaté-Gilarte et al., EPJ Web Conf., 146 08004, (2017)
[5] L. Damone et. al., Phys. Rev. Let., 121, 042701, (2018.)
[6] A. Stamatopoulos et. al., Phys. Rev. C, 102, 014616, (2020)
[7] V. Alcayne et al., EPJ Web Conf., 239 01034 (2020)
[8] A. Oprea et al., EPJ Web Conf., 239 01009. (2020)
[9] R. Plag *et al.*, Nuc. Inst. Meth. A. 496 2, 425-436, (2003)
[10] P.F. Mastinu et al., New C6D6 detectors: reduced neutron sensitivity and improved safety. n_TOF-PUB-2013-00 (2013)
[11] V. Alcayne et al. PhD Thesis. CERN-THESIS-2022-060. (2022)
[12] S. Agostinelli et al., Nucl. Instrum. Meth. A 506, 250 (2003)
[13] A. Plompen et al., Eur. Phys. J. A 56, 181 (2020)
[14] J.A. Pavón et al., Characterisation of the n_TOF 20 m beam line at CERN with the new spallation target (2022), ND2022 Conference, EPJ Web of Conferences.
[15] J. Balibrea-Correa et al., Tech. rep., CERN-INTC-2020-062.
[16] J. Lerendegui-Marco et al., Tech. rep., CERN-INTC-2020-065;